ELSEVIER

Thermochimica Acta 379 (2001) 111–115

thermochimica acta

www.elsevier.com/locate/tca

# Molybdenum species identification on pillared clays by temperature-programmed reduction

P. Salerno*, M.B. Asenjo, S. Mendioroz

*Instituto de Catálisis y Petroleoquímica (CSIC), Cantoblanco, 28049 Madrid, Spain*

**Abstract**

In order to use pillared clays (PILCs) as a support for HDS catalysts, a work was undertaken on which the effect of the support on creation and distribution of species was studied. As a support, aluminum-pillared clay (Al-PILC) and different precursors and loading conditions were used. Temperature-programmed reduction (TPR) and UV-diffuse reflectance (UV-DRS) techniques were applied to identify the formed species. © 2001 Elsevier Science B.V. All rights reserved.

*Keywords:* PILCs; TPR; UV-DRS; Molybdenum catalyst

## 1. Introduction

In preparing HDS catalysts, TPR is an important tool to characterize the wide range of species resulting from varying the conditions of molybdenum incorporation to supports.

As it is commonly admitted [1], pure bulk oxides reduce at higher temperature than supported ones. This fact was interpreted, as the size of supported crystallite being much smaller than the bulk crystals. Shifts in the starting reduction temperature are understood as changes in the crystallite size, but also, in the intensity of the interaction between active phase and support.

On the other hand, supported oxides exposed to ambient conditions assume different species as they were in liquid phase at a pH determined by the point of zero surface charge (PZSC) of the components: active phase and support [2]. Since clays have tetrahedral silica as main component, their isoelectric point should be around 2 and Mo is expected to be as polymolybdate. However, the presence of $Al_2O_3$ (constituting the coordinatively unsaturated cations at the edges of the octahedral layer of the clay lamellae and the pillaring cations in the interlayer), modify the isoelectric point to values slightly higher than 3 and, consequently, species other than polymolybdate could be expected.

In this work, we pretend to discern the effect of the support on formation and distribution of molybdenum species, under different precursors and loading conditions. To achieve that, TPR analysis was used, showing its usefulness as a characterization technique on this field.

## 2. Experimental

The X-ray powder diffraction (XRD) analysis were recorded with a SEIFERT-XRD3000 diffractometer at a scan rate of $0.02^\circ$ $2\theta$/min, 5 s/step accumulation time and a monochromatic Cu K$\alpha$ radiation.

The BET specific surface, volumes of micro- and meso-pores were obtained from $N_2$ adsorption–desorption isotherms at 77 K, measured in a Micromeritics

* Corresponding author. Tel.: +34-1-5854794/ext. 4875; fax: +34-1-5854760.
*E-mail address*: patty@icp.csic.es (P. Salerno).


PII: S0040-6031(01)00609-8

ASAP 2000. Macro-pores determination was performed in a Fisons mercury intrusion apparatus (Pascal 140 and Pascal 240).

TPR analysis was performed in an own made apparatus consisted of a 6 mm (o.d.) quartz tube online with a thermal conductivity detector. Temperature was applied through a temperature control unit with ±2 K precision. Thermoreduction tests were performed at 25 $cm^3$/min flow rate (15% $H_2$) and 10 K/min heating rate upto 1273 K.

UV-DRS spectra of powered samples were collected in a Shimadzu UV-2100 spectrophotometer model GDU-20C, and results expressed as a Kubleka–Munk–Schuster function between 200 and 600 nm.

### 2.1. Support preparation

PILCs were prepared from a 50% natural clay suspension (from La Serrata de Nijar, Spain) in acetone using, as pillaring agent, a 50% aqueous solution of Locron® (a form of Al Keggin cation commercialized by Hoechst) with a 30 meq./g clay ratio [3]. After washing until chloride free and drying at 333 K, the pillars were fixed at 773 K for 2 h. The pillared material was labeled as Loc30. This material increases upto 75% the $Al_2O_3$ content in the parent clay (see Table 1), has a basal spacing, measured by XRD, of 18 Å (that represents an increase of interlamellar spacing of 9 Å over the dehydrated parent clay), a BET surface area of 320 $m^2$/g and a micro-pore volume of 0.090 $cm^3$/g.

### 2.2. Catalyst preparation

The active phase was incorporated to the pillared clay by two methods: incipient wetness in aqueous solution (pH = 10) of ammonium heptamolybdate (AHM) and physical mixture of appropriate amounts of $MoO_3$ and clay components in *n*-heptane by 5 min ultrasonic bath. After impregnation or mixing, the materials were dried 24 h at room temperature and then heat-treated at 773 K for 4 h.

The impregnated samples were labeled as Mo(3)/Loc30 and Mo(12)/Loc30, and the mixed ones as Mo(3) + Loc30 and Mo(12) + Loc30, where the number inside the parenthesis shows the $MoO_3$ percent weight by mass unit of support. Molybdenum loading was calculated in order to obtain 0.4 and 1.2 Mo atoms/$nm^2$ of support, respectively.

Bulk $MoO_3$ was prepared by heating pure AHM at 773 K, 8 h. This powdered material was also used as a reference for peaks assignation on TPR experiments.

## 3. Results

Tables 1 and 2 shows the major characteristics of the prepared catalyst obtained by the techniques described above.

Table 1
Elemental composition of materials (expressed as oxide wt.%)

| Material | $Al_2O_3$ | CaO | $Fe_2O_3$ | $K_2O$ | MgO | MnO | $Na_2O$ | $SiO_2$ | $H_2O$ | Total |
|---|---|---|---|---|---|---|---|---|---|---|
| Natural clay | 17.8 | 1.6 | 2.63 | 0.65 | 5.17 | 0.04 | 1.09 | 61 | 12.6 | 100.0 |
| Loc30 | 31.2 | 0.17 | 2.38 | 0.43 | 3.93 | 0.03 | 0.12 | 57 | 5.3 | 101.3 |

Table 2
Physico-chemical properties of the samples

| Catalyst | $S_{BET}$ ($m^2$/g) | Is $d_{0\,0\,1}$ stable?[a] | $MoO_3$ by XRD |
|---|---|---|---|
| Loc30 | 320 | – | – |
| Mo(3)/Loc30 | 219 | Yes | No |
| Mo(12)/Loc30 | 202 | Yes | No |
| Mo(3) + Loc30 | 147 | Yes | Weak |
| Mo(12) + Loc30 | 194 | Yes | Strong |

[a] Is support $d_{0\,0\,1}$ still visible after molybdenum incorporation?

### 3.1. X-ray diffractograms

It can be notice in Table 2 that mixed samples show diffraction lines corresponding to $MoO_3$, whereas the impregnated ones do not, independently of its molybdenum loading. It should be related with a higher dispersion of molybdenum on the surface of the former. Besides, no changes on basal spacing were noted by X-ray diffractograms, showing that Loc30 was stable under impregnation conditions (basic medium, and heat treatment).

### 3.2. TPR curves

TPR profiles of all samples are gathered in Fig. 1. Also, bulk $MoO_3$ from pure AHM, under the conditions said above, has been included in the figure as a reference to assign the peaks corresponding to Mo species on supported samples. From them, it can be seen that: (1) although the profiles of the samples are roughly similar and follow the pattern of bulk $MoO_3$, with two reduction steps at low- and high-temperature, the peak intensities change with the precursor. On impregnated samples, the high-temperature peak decreases, in Mo(12)/Loc30, or disappears, in Mo(3)/Loc30, with regard to the low-temperature one, whereas on mixed ones the opposite happens showing a profile alike bulk $MoO_3$; (2) the reduction process starts at considerably lower temperature on all supported materials than on bulk oxide; (3) the reduction degree of the supported samples is always lower than theoretical, and decreases with metal content; (4) also, the reduction degree of impregnated catalysts is lower than that of the mixed ones. That means a stronger interaction between Mo and the support surface after impregnation.

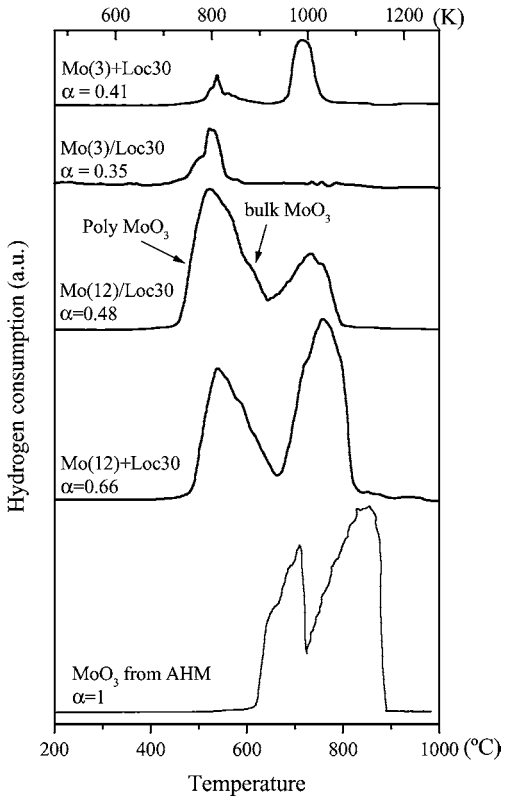


Fig. 1. TPR of impregnated and mixed catalysts.

### 3.3. UV-DRS spectra

UV-DRS spectra are shown in Fig. 2. All samples except Mo(3)/Loc30 contain a strong band centered around 400 nm showing the presence of octahedrally coordinated Mo. Impregnated samples show besides a second band between 230 and 240 nm assigned to tetrahedral Mo [4]. Finally, one more band at 275 nm appeared on Mo(3)/Loc30 which has been associated to octahedral molybdenum.

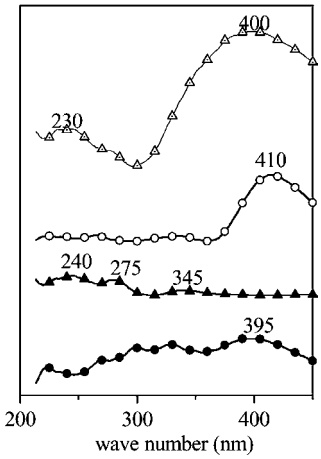


Fig. 2. UV-diffuse reflectance of impregnated (triangles) and mixed (circles) catalyst: (△) Mo(12)/Loc30; (○) Mo(12) + Loc30; (▲) Mo(3)/Loc30; (●) Mo(3) + Loc30.

## 4. Discussion

The fact that the reduction starts at a considerably lower temperature on supported materials with respect to bulk oxide, denotes a considerable dispersion of the precursor on the support surface [1,5], confirming results from X-ray diffractograms.

As expected, the high-temperature reduction peak is higher on the mixed than on the impregnated catalysts showing a smaller metal–support interaction.

The reduction degree is small in all catalysts. As it is known, $MoO_3$ completely reduces when mixed with $SiO_2$, but not with $Al_2O_3$ [5], which has been related to a stronger interaction of Mo species with the latter. If so, Al-PILC behaves more like alumina than like silica with respect to Mo species. Alumina addresses the clay interaction with Mo, because: (1) it takes part of the coordinatively unsaturated cations (CUS) of the octahedral layer in the clay which are more reactive [6]; (2) it creates pillars giving rise to narrow pores with enhanced interaction potential [7]; (3) there is an excess alumina (∼5%) on the clay surface, becoming from the Al/clay ratio used on Al-PILC synthesis process, more accessible to Mo than the silica underneath and; (4) the local PZSC of alumina, around 8, helps the incorporation of anionic molybdenum to restricted patches of the sample [8].

On alumina, Mo can exist as a monomer at low loading and as polymolybdate at high loading [5]. The same happens when using Al-PILCs as a support, as has been supported by UV-DRS through the 230 nm peak on impregnated samples, commonly assigned to monomeric species [9], and is also consistent with their low reducibility, which decreases with Mo loading.

Apart from this irreducible fraction of Mo, two peaks are expected in the reduction process [5] as said above; however, a third peak overlapping the low-temperature peak is visible in all samples impregnated or mixed, more in those with high Mo content. This ''spurious'' peak must be ascribed to a second species associated to the main species, which is strictly related to the precursor nature. Since it also appears on mixed samples, an additional action from the support acid–base character on the original species must be admitted. This acid–base character, magnified in aqueous solution, acts through ambient air exposure and changes the equilibrium among Mo species [2].

The same behavior is visible on samples with low Mo content. On sample Mo(3)/Loc30, only a small low-temperature peak with two components is visible, due to polymeric Mo and $MoO_3$ reduction. The effect of support interaction with such a low Mo content is enhanced and reduction from $Mo^{4+}$ to $Mo^0$ does not take place. In contrast, on Mo(3)+ Loc30, the low-temperature peak, is practically negligible, although, it still denotes the presence of a second component, and the smaller interaction with the mixed $MoO_3$ is shown in the high-temperature peak detected.

In our opinion, a number of acid sites on the solid surface in presence of humidity interact with Mo species upto a limit and modifies the Mo precursor, giving rise to surface molybdate structure. This humidity might become either from the impregnating solution or from surface re-hydration at room conditions [1,2]. PILC acidity effect leads towards $MoO_3$ formation, where final structure is more visible on samples becoming from AHM and impregnation.

## 5. Conclusion

TPR has shown as a useful technique to characterize Mo surface species. Al-PILC used as support to molybdenum, behaves, under work conditions here, as alumina toward Mo species formation. That suggests that Al-PILCs could be used as HDS support.

The generated species by different incorporation methods might be modified under ambient conditions in function of support–metal interactions. The molybdate–support interaction for hydrated samples is therefore determined by the solid PZSC.

## References

[1] P. Arnoldy, J.C.M. Jonge, J.A. Moulijn, J. Phys. Chem. 89 (1985) 4517.
[2] C.C. Williams, J.G. Ekerdt, J. Jehng, F.D. Hardcastle, I.E. Wachs, J. Phys. Chem. 95 (1991) 8781.
[3] L. Storaro, M. Lenarda, R. Ganzerla, A. Rinaldi, Microporous Mater. 6 (1996) 55.

[4] N. Arul Dhas, A. Gedanken, J. Phys. Chem. 101 (1997) 9495.
[5] J.R. Regalbuto, J.W. Ha, Catal. Lett. 29 (1994) 189.
[6] H. Ming Yuan, L. Zhonghui, M. Enze, Catal. Today 2 (2/3) (1988) 321.
[7] S.J. Gregg, K.S.W. Sing (Eds.), Adsorption, Surface Area and Porosity, Academic Press, New York, 1982.
[8] R. López Cordero, F.J. Gil Llambias, A. López Agudo, Appl. Catal. A 74 (1991) 125.
[9] R. Kumar Rana, B. Viswanathan, Catal. Lett. 52 (1998) 25.